POLITECNICO
MILANO 1863

DIPARTIMENTO DI MECCANICA

mecc

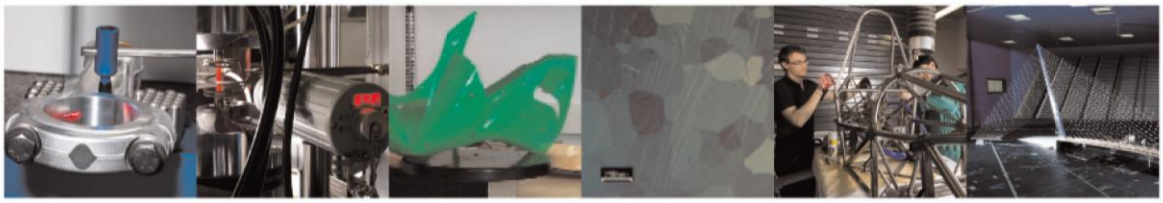

A novel harmonic solution for chatter stability of time periodic systems

Defant, F.; Albertelli, P.

This is a post-peer-review, pre-copyedit version of an article published in JOURNAL OF SOUND AND VIBRATION. The final authenticated version is available online at: http://dx.doi.org/10.1016/j.jsv.2020.115719

This content is provided under CC BY-NC-ND 4.0 license

DIPARTIMENTO DI MECCANICA ■ POLITECNICO DI MILANO
via G. La Masa, 1 ■ 20156 Milano ■ EMAIL (PEC): pecmecc@cert.polimi.it
http://www.mecc.polimi.it
Rev. 0

A Novel Harmonic Solution for Chatter Stability of Time Periodic Systems

Fabrizio Defant[a,1,*], Paolo Albertelli[b]

[a] *R&D Department, Pama S.p.A, Viale del Lavoro 10, 38068 Rovereto (TN), Italy*
[b] *Mechanical Engineering Department, Politecnico di Milano, Via La Masa 1, 20156 Milano, Italy*

Abstract

Chatter vibrations strongly limit productivity in milling. Due to the presence of rotating parts with asymmetric stiffness and stability enhancement strategies which act through a periodic variation of stiffness, there is growing interest in estimating the stability maps of systems with Linear Time Periodic dynamics together with periodic cutting excitation. Applying Exponentially Periodic Modulated test signals to the dynamic cutting force equation and representing the dynamics of the system through the Harmonic Transfer Function, the innovative Harmonic Solution (HS) and its zero-order approximation were derived in this research. HS is a frequency domain representation of a system described by the combination of two independent periodicities. It is possible to take into account these periodicities together in HS or singularly, resulting in the Zero Order HS or in the well-known Multi-Frequency Solution. This novel formulation can deal efficiently with spindle dependent and independent dynamics and is prone to industrial applications due to its flexibility and efficiency. More specifically, in this work the developed methodologies were used to assess the cutting stability of systems with a periodically modulated stiffness. The accuracy and efficiency of HS were validated by comparison with the results

*Corresponding author
Email addresses: fabrizio.defant@pama.it (Fabrizio Defant), paolo.albertelli@polimi.it (Paolo Albertelli)
[1] Executive PhD Candidate at Mechanical Engineering Department, Politecnico di Milano, Via La Masa 1, 20156 Milano, Italy

achieved by the use of the semi-discretization method. Results are in agreement with those obtained using semi-discretization. Moreover, admitting a slight precision loss, HS and its zero-order approximation are orders of magnitude faster than semi-discretization, giving reliable stability maps from seconds to a few minutes.
Keywords: linear stability, chatter, time delay, linear time periodic systems, stiffness variation

1. Introduction

Chatter is an ancient but still current problem facing machinists, which is the first limitation for machining productivity and cost reduction. The most common mechanism of chatter is the regeneration of chip thickness. Vibrations between tool and workpiece leave a wavy surface after a tooth pass, which is cut again by the subsequent tooth. Therefore, the chip thickness and the cutting force vary causing system instability. By increasing the depth of cut, the modulation leads to strong self-excited vibrations, which are detrimental to both the quality of the processed workpiece and the health of the machine tool. The prediction of stability maps given as function of the spindle speed (Ω) and depth of cut (a) covers a crucial role while planning machining operations. Those maps are known as stability lobes diagrams, which can be estimated through time domain (i.e. Semi-discretization [1, 2], Full-discretization [3] and others [4, 5]) and frequency domain techniques (e.g. Zero Order Approximation Solution [6], Multi Frequency Solution [7] and other extensions [8, 9]). Time domain techniques are based on the Floquet theory, where the eigenvalues of the matrix which links the state at time t_0 and one period later $t_0 + T$ (i.e. monodromy matrix) give the properties of stability. For time delayed systems the monodromy is infinitely dimensional, therefore techniques aim to achieve reduction to a finite problem, without losing stability information. Those methods can take into account different types of delay and periodicity of the system, however they are generally time consuming. On the other hand, frequency domain tech-

niques consider the delay as a feedback control loop. Consequently, the stability limit is studied by solving the characteristic equation of the closed loop system. These strategies are generally efficient and find their practical application in industry with good results. However, approximations of the dynamics and of the time delay are taken into account. Considering the neglected aspects may be intricate and usually leads to losing the generality of the approach.

The stability analysis of systems with linear time periodic (LTP) dynamics has gained interest, and consequently the estimation of stability lobes diagrams under this assumption. The main source of periodicity is given by the rotation of the tool. The first consequence is that the cutting force rotates with it, thus the directional cutting force coefficients vary periodically [10]. Moreover, the presence of asymmetric stiffness of rotating parts [11] (i.e. two fluted end mills) or of the workpiece [12] (i.e. thin wall) introduce LTP dynamics. These problems were solved by means of changing the coordinates from stationary to rotational in the frequency domain, which leads to a linear time invariant (LTI) but speed dependent system. In the presence of combined stationary and rotating asymmetric stiffness, an extension of the Multi Frequency Solution was developed by Mohammadi and Ahmadi [9]. It takes into account systems with LTP dynamics the period of which is a small multiple of the spindle rotation. Moreover, a novel strategy to increase the stability limit, known as stiffness variation, works by periodically varying the stiffness of the system with a period that is independent from the spindle rotation. The stability was first studied by Segalman and Redmond [13] by means of numerical integration of the Delay Differential Equation at particular points of the stability lobes diagram. Then, studies was mainly focussed on the turning operation where the stability is studied based on harmonic balance [14], temporal finite element techniques [15], an energy approach [16] and an averaging method [17]. However, the last works deal with full-discretization approximating the delay term using Hermite [18] and Lagrange [19] interpolation and semi-discretization in a milling application [20, 21]. Semi-discretization gives accurate results, however it is time consuming and the identification of the modal parameters is needed. The computational

time depends on the Floquet (fundamental) period, which may be thousands times the stiffness variation period under these assumptions. Therefore, the solution time may be extremely long. Moreover, taking into account systems with multiple critical modes will increase the complexity, and thus the computational effort.

In this paper, the Harmonic Solution (HS) and Zero Order Harmonic Solution (ZOHS) are developed efficiently to take into account the LTP dynamic in the frequency domain. The Harmonic Solution (HS) is obtained applying the theory of LTP systems developed by Wereley [22]. Thus, Exponentially Periodic Modulated (EMP) signals and harmonic balance are applied to the dynamic cutting force in milling. In LTP dynamics, the Harmonic Transfer Function (HTF) plays the role of Frequency Response Function (FRF). It is shown that HTF also deals with LTI systems and the novel formulation gives a new perspective to the existing LTI techniques. Indeed, the Multi Frequency Solution [7] can be written in terms of the HTF. Furthermore, the zero order approximation of HS (truncation considering zero harmonics) is Altintas's Zero Order Approximation solution [6]. The HS converges rapidly when the dynamics vary according to the spindle speed rotation. However, when it is due to a constant frequency of stiffness variation the number of harmonics which must be taken into account in order to assure an accurate estimation of the stability lobes diagram grows, which leads to long computational time. Thus the ZOHS was developed, which only considers the constant value of the cutting force as in [6], but includes the harmonics due to the variation of the dynamics (i.e. HTF). It was shown that the ZOHS gives accurate results by order of magnitude faster than semi-discretization. Overall, this can be a suitable tool for application in industry and for conducting efficient optimization of stiffness variation parameters.

This paper is organized as follows: in Section 2 the dynamic milling equation and the representation of LTP dynamics in frequency domain are introduced. In Section 3 the HS was derived and it is shown how by managing the content of the directional matrix and HTF it is possible to reproduce the Multi Frequency Solution formulation [7] and the novel ZOHS. Finally, in Section 4 HS and ZOHS

were validate through semi-discretization and the enhancement of the stability limit due to stiffness variation is evaluated.

2. Materials and methods

2.1. Dynamic Equation of Milling with Stiffness Variation

A 2-dof model is taken into account, where the stiffness is modulated according to a given function. For the sake of generality, the mass and damping are also considered to be time periodic.

$$\mathbf{M}(t)\ddot{\mathbf{q}}(t) + \mathbf{C}(t)\dot{\mathbf{q}}(t) + \mathbf{K}(t)\mathbf{q}(t) = \mathbf{F}(t) \tag{1}$$

The left hand side of Eq. (1) contains the $T_{\mathrm{sv}}-$periodic mass $\mathbf{M}(t) = \mathbf{M}(t+T_{\mathrm{sv}})$, damping $\mathbf{C}(t) = \mathbf{C}(t+T_{\mathrm{sv}})$ and stiffness $\mathbf{K}(t) = \mathbf{K}(t+T_{\mathrm{sv}})$ matrices of the system, while on the right hand side there is the cutting force $\mathbf{F}(t)$. Finally, $\mathbf{q}(t)$ is the 2-dof position vector, which consider the two orthogonal direction x and y in the cutting plane (Fig. 1). The cutting force depends on the chip thickness [6], which is given by the difference between position of the current cutter and the previous cutter in the same angular position φ (Fig. 1):

$$h(\varphi_j) = g(\varphi_j)\Big(s_t \sin(\varphi_j) + (v_{j,0} - v_j)\Big) \tag{2}$$

where s_t is the feed per tooth, $(v_{j,0}, v_j)$ are the dynamic displacement of the cutter at the previous and present tooth periods respectively and $g(\varphi_j)$ is a unit step function which determines whether the cutter is in or out of the cut.

$$g(\varphi_j) = \begin{cases} 1 & \text{if} \quad \varphi_{\mathrm{st}} \leq \varphi_j < \varphi_{\mathrm{ex}} \\ 0 & \text{if} \quad \varphi_j < \varphi_{\mathrm{st}} \text{ or } \varphi_j < \varphi_{\mathrm{ex}} \end{cases} \tag{3}$$

The static part $s_t \sin(\varphi_j)$ is neglected because it does not affect the dynamic chip load regeneration mechanism. Thus, by substituting the dynamic displacement the chip thickness reads:

$$h(\varphi_j) = g(\varphi_j)\Big(\Delta x \sin(\varphi_j) + \Delta y \sin(\varphi_j)\Big) \tag{4}$$

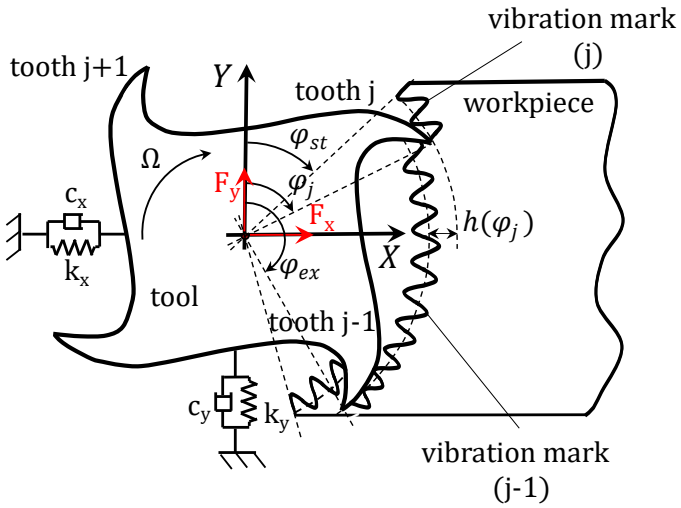

Fig. 1. 2-dof milling model

where $\Delta x = x - x_0$ and $\Delta y = y - y_0$. Finally, the dynamic force is given by:

$$\mathbf{F}(t) = \frac{1}{2} a K_t \mathbf{A}_{\mathrm{D}}(t)\big(\mathbf{q}(t) - \mathbf{q}(t-\tau)\big) \tag{5}$$

where K_t is the tangential cutting force coefficient and $\mathbf{A}_{\mathrm{D}}(t)$ is the $\tau-$periodic directional matrix, the components of which are the time-varying directional dynamic milling force coefficients given in [6]. Finally, the equation of motion reads:

$$\mathbf{M}(t)\ddot{\mathbf{q}}(t) + \mathbf{C}(t)\dot{\mathbf{q}}(t) + \mathbf{K}(t)\mathbf{q}(t) = \frac{1}{2} a K_t \mathbf{A}_{\mathrm{D}}(t)\big(\mathbf{q}(t) - \mathbf{q}(t-\tau)\big) \tag{6}$$

As shown in Eq. (6), the equation of motion which governs the regenerative cutting mechanism in milling is delayed and periodic. The periodicity is given by the lowest common multiple of the tooth passing period τ and the period of stiffness variation T_{sv}, while the force depends on the chip thickness, which is given by the instantaneous and past position of the cutter ($\mathbf{q}(t)$ and $\mathbf{q}(t-\tau)$).

For the sake of simplicity, in the following section a simplified 2-dof stiffness variation model was considered. Only the stiffness was varied about the natural

frequency according to a given function $f_i(t)$ (sine, square, triangle, random, ...) as in [20]. Rearranging and explicating the matrices' components, the equation of motion of the system reads:

$$\ddot{\mathbf{q}}(t) + \begin{bmatrix} 2\zeta_x\omega_{\mathrm{nx}} & 0 \\ 0 & 2\zeta_y\omega_{\mathrm{ny}} \end{bmatrix} \dot{\mathbf{q}}(t) + \begin{bmatrix} \omega_{\mathrm{nx}}^2(1+f_x(t)) & 0 \\ 0 & \omega_{\mathrm{ny}}^2(1+f_y(t)) \end{bmatrix} \mathbf{q}(t) = \\ = \frac{1}{2} a K_t \begin{bmatrix} 1/m_x & 0 \\ 0 & 1/m_y \end{bmatrix} \begin{bmatrix} \alpha_{\mathrm{xx}} & \alpha_{\mathrm{xy}} \\ \alpha_{\mathrm{yx}} & \alpha_{\mathrm{yy}} \end{bmatrix} \big(\mathbf{q}(t) - \mathbf{q}(t-\tau)\big) \quad (7)$$

2.2. Time Periodic Dynamics in the Frequency Domain

The input - output relation for LTP systems cannot be achieved considering complex exponential test signals $u(t) = \mathrm{e}^{st}$. Indeed, when applying $1+a_{\mathrm{sv}} \sin \omega_p t$ to a time periodic gain, the output is given by the sum of three complex exponentials [22]:

$$y(t) = \mathrm{e}^{st} + a_{\mathrm{sv}}\, \mathrm{e}^{(s+\mathrm{i}\,\omega_p)t} + a_{\mathrm{sv}}\, \mathrm{e}^{(s-\mathrm{i}\,\omega_p)t} \quad (8)$$

The output is modulated by the harmonics of the system's fundamental frequency, known as the pumping frequency ω_p. The transfer function in LTI systems maps a sinusoidal frequency input ω signal, into a sinusoidal output signal of the same frequency, but with a possible different amplitude and phase. The same transfer function for LTP systems has been elusive, because it maps a sinusoidal frequency input ω signal, into a multi-sinusoidal $\omega + \mathrm{i}\, n\omega_p$ output, where $n = \ldots, -2, -1, 0, 1, 2, \ldots$. EMP signals $u(t) = \mathrm{e}^{(s+\mathrm{i}\, n\omega_p)t}$ (where $s \in \mathbb{C}$) in LTP systems play the role of a complex exponential in LTI systems, thus it is possible to map the input-output relation as shown in [22] as shown briefly below.

The state space representation of an LTP system relates to Eq. (9) and Eq. (10).

$$\dot{\mathbf{x}}(t) = \mathbf{A}(t)\mathbf{x}(t) + \mathbf{B}(t)\mathbf{u}(t) \quad (9)$$

$$\mathbf{y}(t) = \mathbf{C}(t)\mathbf{x}(t) + \mathbf{D}(t)\mathbf{u}(t) \quad (10)$$

State, input and output are substituted by EMP signals and the matrices are expanded using the Toeplitz transform. The Toeplitz transformation organized the Fourier coefficients of matrices $A(t)$ (computed as in Eq. (19)) into a matrix with a block-Toeplitz form:

$$\mathcal{A} = \begin{bmatrix} \ddots & \vdots & \vdots & \vdots & \iddots \\ \dots & \mathbf{A}_0 & \mathbf{A}_{-1} & \mathbf{A}_{-2} & \dots \\ \dots & \mathbf{A}_1 & \mathbf{A}_0 & \mathbf{A}_{-1} & \dots \\ \dots & \mathbf{A}_2 & \mathbf{A}_1 & \mathbf{A}_0 & \dots \\ \iddots & \vdots & \vdots & \vdots & \ddots \end{bmatrix} \tag{11}$$

The definition is similar for matrices $\mathbf{B}(t)$, $\mathbf{C}(t)$ and $\mathbf{D}(t)$, the Toeplitz transformations of which are $\mathcal{B}$, $\mathcal{C}$ and $\mathcal{D}$. Rearranging the equations as in [22] it is possible to find the link between the Fourier coefficients of the input with those of the output $\mathbf{Y} = \tilde{\mathcal{H}}(s)\mathbf{U}$, which defines the analytical formulation of the HTF (Eq. (12)):

$$\mathbf{Y} = \Big\{ \mathcal{C}[s\mathbf{I} - (\mathcal{A} - \mathcal{N})]^{-1}\mathcal{B} + \mathcal{D} \Big\} \mathbf{U} \tag{12}$$

where $\mathcal{N} = \text{blkdiag}(\mathrm{i}\, n\omega_p \mathbf{I})$, while $\mathbf{Y}$ and $\mathbf{U}$ are the vectors of Fourier coefficients of output and input respectively, which have the form:

$$\mathbf{Y} = \begin{pmatrix} \dots & \mathbf{Y}_{-2} & \mathbf{Y}_{-1} & \mathbf{Y}_0 & \mathbf{Y}_1 & \mathbf{Y}_2 & \dots \end{pmatrix}^\top \tag{13}$$

This formulation is useful to compute the HTF from the state space representation, however it does not give information about the content of HTF elements. Indeed, by expanding the matrix and vectors of Eq. (12), it is possible to see that the elements are independent from each other:

$$\begin{pmatrix} \vdots \\ \mathbf{Y}_{-1} \\ \mathbf{Y}_0 \\ \mathbf{Y}_1 \\ \vdots \end{pmatrix} = \begin{bmatrix} \ddots & \vdots & \vdots & \vdots & \iddots \\ \dots & \mathbf{H}_{-1,-1}(s) & \mathbf{H}_{-1,0}(s) & \mathbf{H}_{-1,1}(s) & \dots \\ \dots & \mathbf{H}_{0,-1}(s) & \mathbf{H}_{0,0}(s) & \mathbf{H}_{0,1}(s) & \dots \\ \dots & \mathbf{H}_{1,-1}(s) & \mathbf{H}_{1,0}(s) & \mathbf{H}_{1,1}(s) & \dots \\ \iddots & \vdots & \vdots & \vdots & \ddots \end{bmatrix} \begin{pmatrix} \vdots \\ \mathbf{U}_{-1} \\ \mathbf{U}_0 \\ \mathbf{U}_1 \\ \vdots \end{pmatrix} \tag{14}$$

A more convenient way to write the input - output relation is based on the impulse response representation [23]. The generic element $H_{n,m}$ acts as a filter and a frequency shift, thus it can be written as:

$$\begin{aligned}\mathbf{Y}_n &= \sum_{n=-\infty}^{+\infty} \mathbf{H}_{n,m}(s)\mathbf{U}_m \\ &= \sum_{n=-\infty}^{+\infty} \mathbf{H}_{n-m}(s - \mathrm{i}\, n\omega_p)\mathbf{U}_m\end{aligned} \tag{15}$$

This form of the HTF matrix is also known as the Frequency-Lifted Transfer Operator, which reads:

$$\begin{pmatrix} \vdots \\ \mathbf{Y}_{-1} \\ \mathbf{Y}_0 \\ \mathbf{Y}_1 \\ \vdots \end{pmatrix} = \begin{bmatrix} \ddots & \vdots & \vdots & \vdots & \iddots \\ \dots & \mathbf{H}_0(s - \mathrm{i}\,\omega_p) & \mathbf{H}_{-1}(s) & \mathbf{H}_{-2}(s + \mathrm{i}\,\omega_p) & \dots \\ \dots & \mathbf{H}_1(s - \mathrm{i}\,\omega_p) & \mathbf{H}_0(s) & \mathbf{H}_{-1}(s + \mathrm{i}\,\omega_p) & \dots \\ \dots & \mathbf{H}_2(s - \mathrm{i}\,\omega_p) & \mathbf{H}_1(s) & \mathbf{H}_0(s + \mathrm{i}\,\omega_p) & \dots \\ \iddots & \vdots & \vdots & \vdots & \ddots \end{bmatrix} \begin{pmatrix} \vdots \\ \mathbf{U}_{-1} \\ \mathbf{U}_0 \\ \mathbf{U}_1 \\ \vdots \end{pmatrix} \tag{16}$$

The H_0 function, which is on the main diagonal of the HTF, links the harmonics of the input with harmonics of the output at the same frequency. Therefore, the dynamics of an LTI system can be represented in terms of a block-diagonal HTF. Conversely, the out-of-diagonal terms link the harmonics of the input with harmonics of the output at different frequencies, which is the characteristic of LTP systems (frequency shift).

For the sake of information, the use of HTF plays a crucial role in applying the method in industries. It can be experimentally identified [24, 25] and the results can be introduced in the algorithm to study the stability without further manipulation, while with time domain techniques the modal parameters are needed. Moreover, the presence of multiple modes does not affect the computational effort. However, those aspects were not dealt with in depth in this paper.

3. Stability Analysis

3.1. Harmonic Solution

The HS is derived starting from the dynamic cutting force of Eq. (5). The EMP signals for the force, the state and the Fourier transformation of the directional matrix at pumping frequency ω_p, which is the greatest common divisor between the tooth pass frequency τ and the frequency of stiffness variation ω_{sv}, are considered in the following equations:

$$\mathbf{F}(t) = \sum_{n=-\infty}^{+\infty} \mathbf{P}_n \, \mathrm{e}^{s_n t} \tag{17}$$

$$\mathbf{q}(t) - \mathbf{q}(t-\tau) = \sum_{m=-\infty}^{+\infty} \mathbf{Q}_m \, \mathrm{e}^{s_m t} \left(1 - \mathrm{e}^{-s_m \tau}\right) \tag{18}$$

$$\mathbf{A}_{\mathrm{D}}(t) = \sum_{n=-\infty}^{+\infty} \mathbf{\Lambda}_n \, \mathrm{e}^{\mathrm{i}\, n\omega_p t} \tag{19}$$

where $s_n = s + \mathrm{i}\, n\omega_p$ and $s \in \mathbb{C}$ and similarly for s_m.
Substituting Eq. (17), Eq. (18) and Eq. (19) in Eq. (5) and rearranging, the equation reads:

$$\begin{aligned}
\sum_{n=-\infty}^{+\infty} \mathbf{P}_n \, \mathrm{e}^{s_n t} &= \frac{1}{2} a K_t \sum_{n=-\infty}^{+\infty} \mathbf{\Lambda}_n \, \mathrm{e}^{\mathrm{i}\, n\omega_p t} \sum_{m=-\infty}^{+\infty} \mathbf{Q}_m \, \mathrm{e}^{s_m t} \left(1 - \mathrm{e}^{-s_m \tau}\right) \\
\sum_{n=-\infty}^{+\infty} \mathbf{P}_n \, \mathrm{e}^{s_n t} &= \frac{1}{2} a K_t \sum_{n=-\infty}^{+\infty} \sum_{m=-\infty}^{+\infty} \mathbf{\Lambda}_n \, \mathbf{Q}_m \left(1 - \mathrm{e}^{-s_m \tau}\right) \mathrm{e}^{s_{m+n} t} \\
\sum_{n=-\infty}^{+\infty} \mathbf{P}_n \, \mathrm{e}^{s_n t} &= \frac{1}{2} a K_t \sum_{n=-\infty}^{+\infty} \sum_{m=-\infty}^{+\infty} \mathbf{\Lambda}_{n-m} \, \mathbf{Q}_m \left(1 - \mathrm{e}^{-s_m \tau}\right) \mathrm{e}^{s_n t}
\end{aligned} \tag{20}$$

The input - output relation can be written in terms of the HTF (Eq. (15)):

$$\mathbf{Q}_m = \sum_{n=-\infty}^{+\infty} \mathbf{H}_{l-m}(s - \mathrm{i}\, l\omega_p)\mathbf{P}_l \tag{21}$$

Then, substituting Eq. (21) in Eq. (20):

$$\sum_{n=-\infty}^{+\infty} \mathbf{P}_n \, \mathrm{e}^{s_n t} = \frac{1}{2} a K_t \sum_{n=-\infty}^{+\infty} \sum_{m=-\infty}^{+\infty} \sum_{l=-\infty}^{+\infty} \mathbf{\Lambda}_{n-m} \mathbf{H}_{l-m}(s - \mathrm{i}\, l\omega_p) \mathbf{P}_l \left(1 - \mathrm{e}^{-s_m \tau}\right) \mathrm{e}^{s_n t} \tag{22}$$

Finally, harmonic balance leads to a set in terms of the following equation:

$$\mathbf{P}_n = \frac{1}{2} a K_t \sum_{m=-\infty}^{+\infty} \sum_{l=-\infty}^{+\infty} \mathbf{\Lambda}_{n-m} \mathbf{H}_{l-m}(s - \mathrm{i}\, l\omega_p) \mathbf{P}_l \left(1 - \mathrm{e}^{-s_m \tau}\right) \tag{23}$$

Managing summations may be cumbersome, therefore the equations are rearranged in Toeplitz notation:

$$\mathbf{P} = \frac{1}{2} a K_t \left(\mathcal{A}_\mathcal{D} - \mathcal{A}_\mathcal{D} \mathcal{E}\right) \tilde{\mathcal{H}} \mathbf{P} \tag{24}$$

where $\mathcal{E} = \mathbf{I}\, \mathrm{e}^{-s_m \tau} = \mathbf{I}\, \mathrm{e}^{-\mathrm{i}(\omega_c + m\omega_p)\tau}$ at the limit of stability and $\mathcal{A}_\mathcal{D}$ is the Toeplitz transformation of the directional matrix $\mathbf{A}_\mathrm{D}(t)$.

Expanding the matrices, HS reads:

$$\begin{pmatrix} \vdots \\ \mathbf{P}_{-1} \\ \mathbf{P}_0 \\ \mathbf{P}_1 \\ \vdots \end{pmatrix} = \frac{1}{2} a K_t \left(\begin{bmatrix} \ddots & \vdots & \vdots & \vdots & \iddots \\ \dots & \mathbf{I} & \mathbf{0} & \mathbf{0} & \dots \\ \dots & \mathbf{0} & \mathbf{I} & \mathbf{0} & \dots \\ \dots & \mathbf{0} & \mathbf{0} & \mathbf{I} & \dots \\ \iddots & \vdots & \vdots & \vdots & \ddots \end{bmatrix} - \begin{bmatrix} \ddots & \vdots & \vdots & \vdots & \iddots \\ \dots & \mathbf{I}\, \mathrm{e}^{-\mathrm{i}(\omega_c - \omega_p)\tau} & \mathbf{0} & \mathbf{0} & \dots \\ \dots & \mathbf{0} & \mathbf{I}\, \mathrm{e}^{-\mathrm{i}\,\omega_c \tau} & \mathbf{0} & \dots \\ \dots & \mathbf{0} & \mathbf{0} & \mathbf{I}\, \mathrm{e}^{-\mathrm{i}(\omega_c + \omega_p)\tau} & \dots \\ \iddots & \vdots & \vdots & \vdots & \ddots \end{bmatrix} \right)$$

$$\begin{bmatrix} \ddots & \vdots & \vdots & \vdots & \iddots \\ \dots & \mathbf{\Lambda}_0 & \mathbf{\Lambda}_{-1} & \mathbf{\Lambda}_{-2} & \dots \\ \dots & \mathbf{\Lambda}_1 & \mathbf{\Lambda}_0 & \mathbf{\Lambda}_{-1} & \dots \\ \dots & \mathbf{\Lambda}_2 & \mathbf{\Lambda}_1 & \mathbf{\Lambda}_0 & \dots \\ \iddots & \vdots & \vdots & \vdots & \ddots \end{bmatrix} \begin{bmatrix} \ddots & \vdots & \vdots & \vdots & \iddots \\ \dots & \mathbf{H}_0(\mathrm{i}\omega_c - \mathrm{i}\omega_p) & \mathbf{H}_{-1}(\mathrm{i}\omega_c) & \mathbf{H}_{-2}(\mathrm{i}\omega_c + \mathrm{i}\omega_p) & \dots \\ \dots & \mathbf{H}_1(\mathrm{i}\omega_c - \mathrm{i}\omega_p) & \mathbf{H}_0(\mathrm{i}\omega_c) & \mathbf{H}_{-1}(\mathrm{i}\omega_c + \mathrm{i}\omega_p) & \dots \\ \dots & \mathbf{H}_2(\mathrm{i}\omega_c - \mathrm{i}\omega_p) & \mathbf{H}_1(\mathrm{i}\omega_c) & \mathbf{H}_0(\mathrm{i}\omega_c + \mathrm{i}\omega_p) & \dots \\ \iddots & \vdots & \vdots & \vdots & \ddots \end{bmatrix} \begin{pmatrix} \vdots \\ \mathbf{P}_{-1} \\ \mathbf{P}_0 \\ \mathbf{P}_1 \\ \vdots \end{pmatrix} \tag{25}$$

3.2. Zero Order Harmonic Solution

The matrices of Eq. (25) have infinite dimension, consequently a truncation of the harmonics is needed to compute the stability map. In practice, according

to Bachrathy [8], a good guess for the number of considered harmonics for LTI systems is $R_{\mathrm{LTI}} = 2\omega_{\mathrm{n,max}}/\Omega$. In the LTP system the pumping frequency ω_p plays the role of the spindle speed Ω. Thus, the truncation number can be expressed as:

$$R_{\mathrm{LTP}} = \frac{2\omega_{\mathrm{n,max}}}{\Omega}\frac{T_p}{\tau} \tag{26}$$

where T_p is the pumping period, τ is the time delay or cutting pass period and $\frac{T_p}{\tau}$ is the Pumping Period to Delay Ratio (PPTDR).
Irrational ratios between stiffness variation period and time delay make the pumping frequency tend towards zero. Therefore, the dimension of the problem increase leading to unfeasible computational time. This means that the behaviour of the LTP system plays a crucial role in the selection of the proper method to determine the stability. The two behaviours considered are:

1. *Constant frequency of stiffness variation*, when the stiffness variation frequency is independent from the spindle speed (which is the case modelled by Wang et al. [20]).
2. *Constant PPTDR*, when the stiffness modulation is due to the spindle rotation [9] (i.e. PPTDR is constant and usually small).

It is possible to efficiently consider HS with a constant PPTDR of up to 3 - 4 (i.e. the number of harmonics needed is 3 - 4 times the LTI case). However, this is still not efficient enough for applications where the stiffness variation frequency is constant. According to Altintas [6], in practical applications the constant value of the directional matrix $\mathbf{A}_{\mathrm{D}}(t) = \mathbf{A}_{\mathrm{D},0}$ is enough to obtain a good approximation of stability lobes diagrams, especially when the radial depth of cut is high. Thus, it is possible to take into account only the average value of the directional matrix and the truncated HTF. As a consequence the dimension of the problem is reduced, because under this assumption the periodicity is only due to the HTF and only its harmonics are taken into account (i.e. $\omega_p = \omega_{\mathrm{sv}}$). Practically, in Eq. (23) $m = n$ is considered, thus only the constant terms Λ_0 are

taken. Rearranging the equation, the Zero Order Harmonic Solution (ZOHS) is given by the following equations.

$$\mathbf{P}_n = \frac{1}{2} a K_t \sum_{l=-\infty}^{+\infty} \mathbf{\Lambda}_0 \mathbf{H}_{l-n}(s - \mathrm{i}\, l\omega_p)\mathbf{P}_l \left(1 - \mathrm{e}^{-s_n \tau}\right) \tag{27}$$

$$\mathbf{P} = \frac{1}{2} a K_t \big(\mathcal{A}_{\mathcal{D},0} - \mathcal{A}_{\mathcal{D},0}\mathcal{E}\big)\tilde{\mathcal{H}}\mathbf{P} \tag{28}$$

$$\begin{pmatrix} \vdots \\ \mathbf{P}_{-1} \\ \mathbf{P}_0 \\ \mathbf{P}_1 \\ \vdots \end{pmatrix} = \frac{1}{2} a K_t \left(\begin{bmatrix} \ddots & \vdots & \vdots & \vdots & \iddots \\ \dots & \mathbf{I} & \mathbf{0} & \mathbf{0} & \dots \\ \dots & \mathbf{0} & \mathbf{I} & \mathbf{0} & \dots \\ \dots & \mathbf{0} & \mathbf{0} & \mathbf{I} & \dots \\ \iddots & \vdots & \vdots & \vdots & \ddots \end{bmatrix} - \begin{bmatrix} \ddots & \vdots & \vdots & \vdots & \iddots \\ \dots & \mathbf{I}\,\mathrm{e}^{-\mathrm{i}(\omega_c - \omega_{\mathrm{sv}})\tau} & \mathbf{0} & \mathbf{0} & \dots \\ \dots & \mathbf{0} & \mathbf{I}\,\mathrm{e}^{-\mathrm{i}\,\omega_c \tau} & \mathbf{0} & \dots \\ \dots & \mathbf{0} & \mathbf{0} & \mathbf{I}\,\mathrm{e}^{-\mathrm{i}(\omega_c + \omega_{\mathrm{sv}})\tau} & \dots \\ \iddots & \vdots & \vdots & \vdots & \ddots \end{bmatrix} \right)$$

$$\begin{bmatrix} \ddots & \vdots & \vdots & \vdots & \iddots \\ \dots & \mathbf{\Lambda}_0 & \mathbf{0} & \mathbf{0} & \dots \\ \dots & \mathbf{0} & \mathbf{\Lambda}_0 & \mathbf{0} & \dots \\ \dots & \mathbf{0} & \mathbf{0} & \mathbf{\Lambda}_0 & \dots \\ \iddots & \vdots & \vdots & \vdots & \ddots \end{bmatrix} \begin{bmatrix} \ddots & \vdots & \vdots & \vdots & \iddots \\ \dots & \mathbf{H}_0(\mathrm{i}\,\omega_c - \mathrm{i}\,\omega_{\mathrm{sv}}) & \mathbf{H}_{-1}(\mathrm{i}\,\omega_c) & \mathbf{H}_{-2}(\mathrm{i}\,\omega_c + \mathrm{i}\,\omega_{\mathrm{sv}}) & \dots \\ \dots & \mathbf{H}_1(\mathrm{i}\,\omega_c - \mathrm{i}\,\omega_{\mathrm{sv}}) & \mathbf{H}_0(\mathrm{i}\,\omega_c) & \mathbf{H}_{-1}(\mathrm{i}\,\omega_c + \mathrm{i}\,\omega_{\mathrm{sv}}) & \dots \\ \dots & \mathbf{H}_2(\mathrm{i}\,\omega_c - \mathrm{i}\,\omega_{\mathrm{sv}}) & \mathbf{H}_1(\mathrm{i}\,\omega_c) & \mathbf{H}_0(\mathrm{i}\,\omega_c + \mathrm{i}\,\omega_{\mathrm{sv}}) & \dots \\ \iddots & \vdots & \vdots & \vdots & \ddots \end{bmatrix} \begin{pmatrix} \vdots \\ \mathbf{P}_{-1} \\ \mathbf{P}_0 \\ \mathbf{P}_1 \\ \vdots \end{pmatrix} \tag{29}$$

3.3. Application to Linear Time Invariant Dynamics

The HS deals directly with systems characterized by LTI dynamics. Under this condition the formulation shows the following properties:

- The FRF evaluated at different harmonics is generalized considering only the diagonal of the HTF.
- The exponential $\mathbf{I}\,\mathrm{e}^{-\mathrm{i}(\omega_c + m\omega_p)\tau} = \mathbf{I}\,\mathrm{e}^{-\mathrm{i}\,\omega_c \tau}$ because the pumping frequency is the cutting pass frequency, which is simplified by the delay τ.

This formulation leads to the Multi Frequency Solution [7] in Eq. (30).

$$\begin{pmatrix} \vdots \\ \mathbf{P}_{-1} \\ \mathbf{P}_0 \\ \mathbf{P}_1 \\ \vdots \end{pmatrix} = \frac{1}{2} a K_t \left(\mathbf{I} - \mathbf{I}\, \mathrm{e}^{-\mathrm{i}\,\omega_c \tau} \right) \begin{bmatrix} \ddots & \vdots & \vdots & \vdots & \iddots \\ \dots & \mathbf{\Lambda}_0 & \mathbf{\Lambda}_{-1} & \mathbf{\Lambda}_{-2} & \dots \\ \dots & \mathbf{\Lambda}_1 & \mathbf{\Lambda}_0 & \mathbf{\Lambda}_{-1} & \dots \\ \dots & \mathbf{\Lambda}_2 & \mathbf{\Lambda}_1 & \mathbf{\Lambda}_0 & \dots \\ \iddots & \vdots & \vdots & \vdots & \ddots \end{bmatrix}$$
$$\begin{bmatrix} \ddots & \vdots & \vdots & \vdots & \iddots \\ \dots & \mathbf{H}_0(\mathrm{i}\,\omega_c - \mathrm{i}\,\omega_t) & \mathbf{0} & \mathbf{0} & \dots \\ \dots & \mathbf{0} & \mathbf{H}_0(\mathrm{i}\,\omega_c) & \mathbf{0} & \dots \\ \dots & \mathbf{0} & \mathbf{0} & \mathbf{H}_0(\mathrm{i}\,\omega_c + \mathrm{i}\,\omega_t) & \dots \\ \iddots & \vdots & \vdots & \vdots & \ddots \end{bmatrix} \begin{pmatrix} \vdots \\ \mathbf{P}_{-1} \\ \mathbf{P}_0 \\ \mathbf{P}_1 \\ \vdots \end{pmatrix} \tag{30}$$

Furthermore, considering zero harmonics, Eq. (25) reduces to Altinta's Zero Order Approximation solution [6]:

$$\mathbf{P}_0 = \frac{1}{2} a K_t \left(1 - \mathrm{e}^{-\mathrm{i}\,\omega_c \tau}\right) \mathbf{\Lambda}_0 \mathbf{H}_0(\mathrm{i}\,\omega_c) \mathbf{P}_0 \tag{31}$$

3.4. Roots computation

The stability is determined through the roots of the characteristic equation. Its formulation depends on the properties of the dynamical system and the desired approximation of the directional matrix. The flowchart in Fig. 2 helps in the selection of the proper formulation. Once the characteristic equation is defined a root finding problem has to be solved in order to draw the stability lobes diagram. When dealing with LTP systems the roots are given by the nontrivial solutions of Eq. (24) and Eq. (28) for the HS and the ZOHS respectively. The determinant of the characteristic equation is written in terms of the HS for the sake of generality:

$$\det\left(\mathbf{I} - \frac{1}{2} a K_t \left(\mathcal{A}_\mathcal{D} - \mathcal{A}_\mathcal{D}\mathcal{E}\right)\tilde{\mathcal{H}}\right) = D(a, \Omega, \omega_c) = 0 \tag{32}$$

The roots finding problem of Eq. (32) is a system of 2 equations (i.e. real and imaginary part) and 3 variables (i.e. depth of cut a, spindle speed Ω and chatter

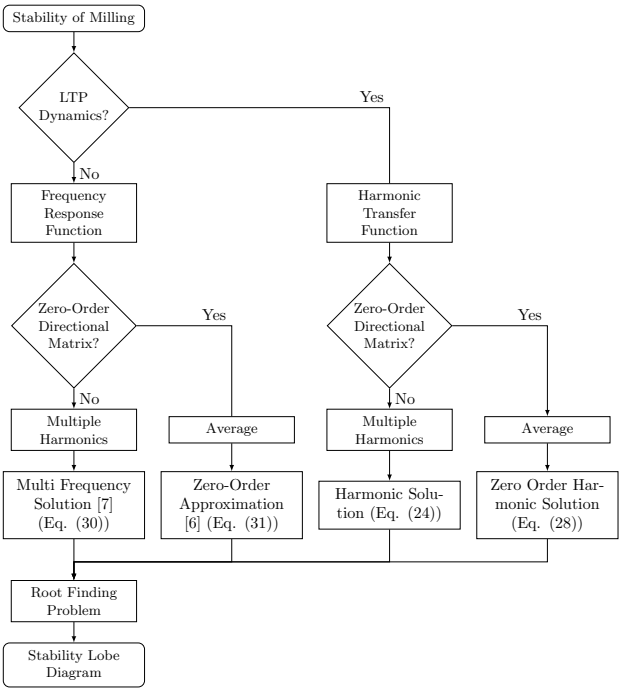

Fig. 2. Selection of the proper characteristic equation formulation and computation of the Stability Lobes Diagram

frequency ω_c). This has been solved through an efficient strategy known as the Multi-Dimensional Bisection Method [26]. It needs an initial mesh, which is related to the desired spindle speed range and the expected depth of cut. Moreover, the chatter frequency range must be defined, which is the most critical part. Practically, good results were obtained considering chatter frequencies at around the critical mode, with amplitude equal to the pumping frequency $[\omega_n - \frac{\omega_p}{2}, \omega_n + \frac{\omega_p}{2}]$. In the end, the lower envelope covering all the roots in terms of depth of cut in 3-dimensional space is taken to be the stability limit. The presence of closed areas in stable or unstable regions represents and island of instability or stability respectively.

4. Results and Discussion

In this section the HS and ZOHS were applied to the model of Eq. (7) to determine the stability lobes diagram. HS and ZOHS deal with the constant PPTDR and constant frequency stiffness variation respectively. Both cases were treated by first considering a convergence analysis to evaluate the proper number of harmonics to take into account and determine the computational effort (Table 1). Then, the methods were validated by comparing the results obtained through semi-discretization (Table 2). Finally, the stability enhancement compared to the equivalent LTI system was evaluated over a wide spindle speed range (Table 3).

The milling of an aluminium alloy was taken into account, the parameters of which were defined in accordance with [20] as follows: the number of teeth is $N = 2$, cutting force coefficients are $K_t = 600$ MPa and $K_n = 200$ MPa, the radial depth of cut is $a_D = 0.1$ and down-milling is adopted. The modal masses are $m_x = m_y = 0.03993$ kg, the natural frequencies are $\omega_{\mathrm{n,x}} = \omega_{\mathrm{n,y}} = 922$ Hz and the damping ratios are $\zeta_x = \zeta_y = 0.011$.

4.1. Constant frequency stiffness variation - ZOHS

Constant frequency stiffness variation is important due to the work of Wang et al. [20], where a wide range of stiffness variation parameters (i.e. frequency, amplitude, function of stiffness variation) were considered with the purpose of optimization within a narrow spindle speed range. ZOHS validation takes into account a constant stiffness variation frequency $\omega_{\mathrm{sv}} = 50$ Hz and relative amplitudes $a_{\mathrm{sv,x}} = a_{\mathrm{sv,y}} = 0.1$. The modulation functions considered are sinusoidal (Eq. (33)) and piece-wise constant (Eq. (34)).

$$f(t) = a_{\mathrm{sv}} \sin(\omega_{\mathrm{sv}} t) \tag{33}$$

$$f(t) = a_{\mathrm{sv}} \operatorname{sgn}\big(\sin(\omega_{\mathrm{sv}} t)\big) \tag{34}$$

The convergence analysis is shown in Fig. 3 considering a sinusoidal stiffness variation function. When $R = 0$ is taken, which is equivalent to the Zero Order

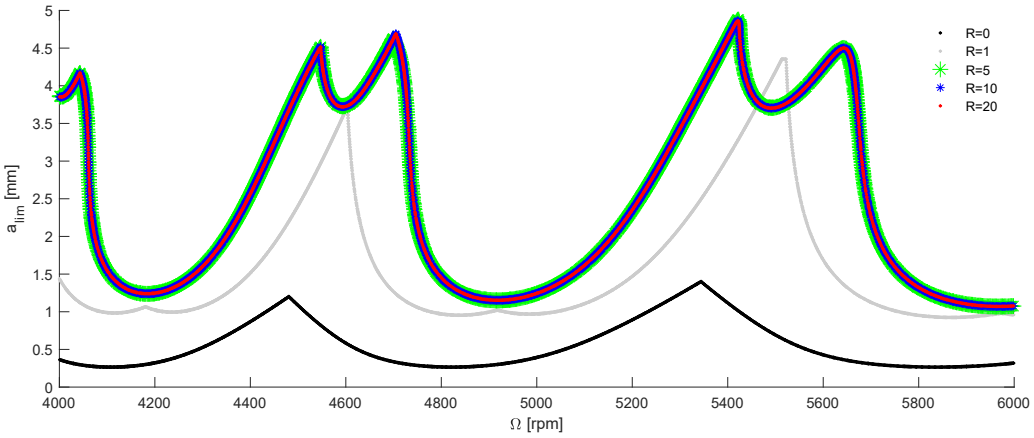

Fig. 3. Convergence analysis of ZOHS with constant frequency stiffness variation (Eq. (28))

Approximation solution [6], the solution does not give information about LTP behaviour. Thus, the number of harmonics considered was increased and the computational time increases as shown in Table 1. Considering $R = 1$ the absolute limit of stability is closer to the actual value and the solution converges with 5 harmonics (green line).

The validation of ZOHS is given in Fig. 4 and Fig. 5, which show the stability lobes diagrams for a sinusoidal and a piece-wise constant function of stiffness variation respectively. The blue line was computed using ZOHS, while the red line is the reference case computed using semi-discretization. The discretization factor taken into account in semi-discretization is $k = 90$, while ZOHS approximates the solution with $R = 10$ harmonics. ZOHS neglects the harmonics of the cut passing frequency, indeed the flip bifurcations at about 5200 rpm are missing in both cases, together with the island of instability at about 4800 rpm in the piece-wise constant modulation case (Fig. 5). In any case, the results are in good agreement in terms of the lobes' shape and position and the absolute limit of stability. Moreover, ZOHS is more efficient, indeed semi-discretization takes about 38 hours, while ZOHS gives excellent results in 55 s, as shown in Table 2. The greater computational efficiency is due to the harmonics truncation, because only those that affect the stability can be taken into account. As a

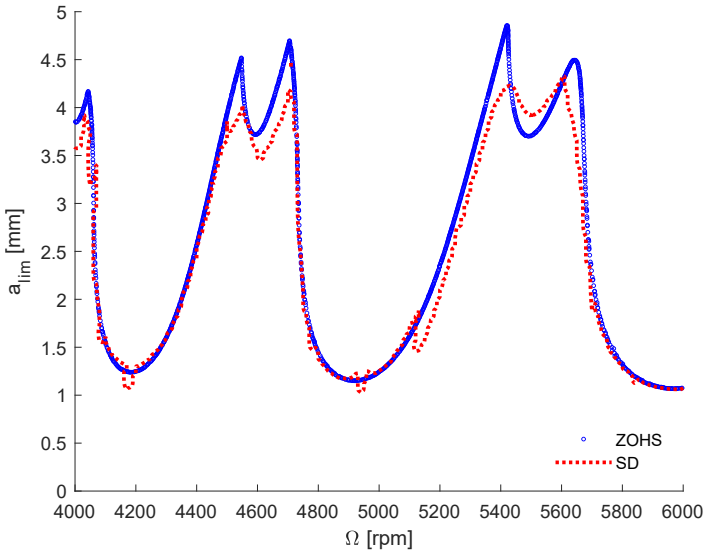

Fig. 4. Validation of ZOHS with sinusoidal function and constant frequency stiffness variation

consequence, ZOHS can cover an important role in industrial applications and for further evaluation and optimization of stiffness variation parameters (i.e. frequency, amplitude, function of stiffness variation).

The efficiency of ZOHS makes it possible to consider a wider spindle speed range with a negligible increase of the computational time. Therefore, the analysis is extended to evaluate the constant frequency stiffness variation at lower spindle speeds. The black line in Fig. 6 shows the stability lobes diagram of the equivalent LTI system computed using the Multi Frequency Solution, while the blue and red path represent the stability lobes diagrams considering sinusoidal and piece-wise constant function of stiffness variation respectively. The technique shows the maximum increase of stable depth of cut in terms of the absolute limit of stability at low cutting speeds, the results of which are summarized in Table 3. The major effect is given while modulating through the piece-wise constant function. The stable depth of cut almost tripled in the piece-wise constant function case, however it needs an instantaneous variation of the dynamic properties which is unrealistic. Therefore, the result produced by considering the sinusoidal stiffness variation is closer to what can be achieved

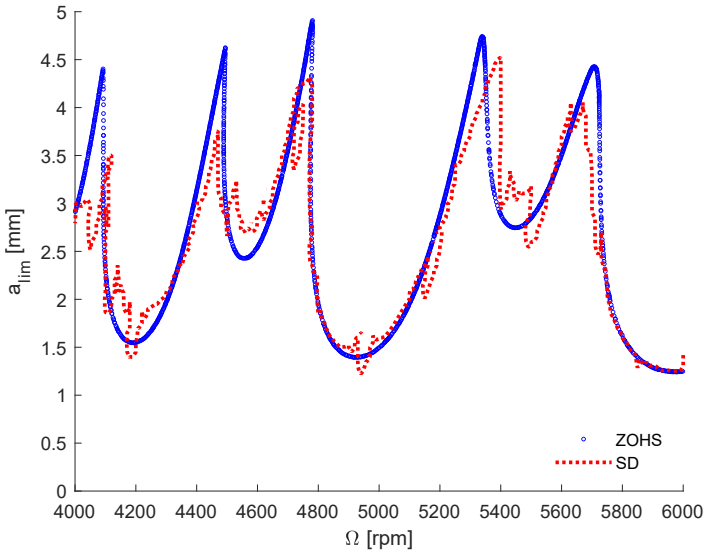

Fig. 5. Validation of ZOHS with piece-wise constant function and constant frequency stiffness variation

in practice. Overall, constant frequency stiffness variation has the greatest potential at medium - low cutting speed, consequently it can find its application in milling of materials characterized by a low cutting speed (e.g. steel and titanium).

4.2. Constant PPTDR - HS

Constant PPTDR is characteristic of those applications where stiffness variation is due to the spindle rotation and is usually characterized by a small and integer PPTDR. This application fits with the characteristic of HS, consequently a precise evaluation of the stability lobes diagrams is possible. The evaluation of its efficiency and accuracy considers a constant PPTDR $\frac{T_p}{\tau} = 2$ and a sinusoidal function of stiffness variation (Eq. (33)) with relative amplitude $a_{\mathrm{sv,x}} = a_{\mathrm{sv,y}} = 0.1$.

The convergence of this method with the number of harmonics is studied and results are shown in Fig. 7. Considering $R = 0$ the method converges quickly to the Zero Order Approximation solution [6] for the equivalent LTI system. The

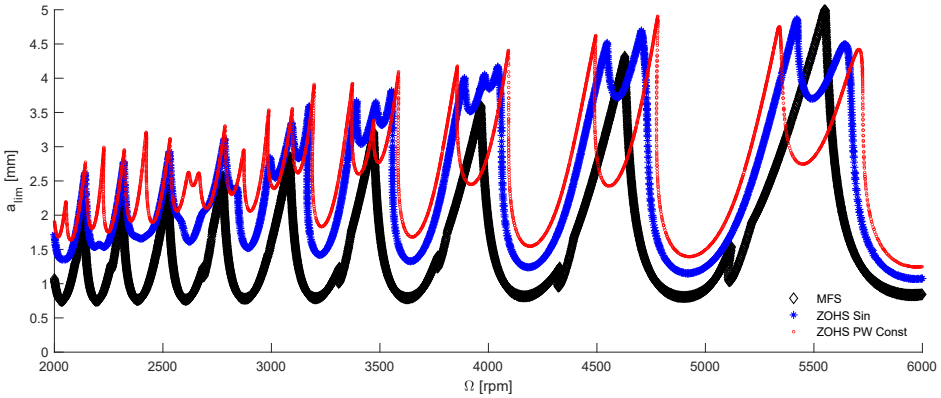

Fig. 6. Stability enhancement of constant frequency stiffness variation

Table 1: Computational time considering an increasing number of harmonics

	ZOHS	HS
R	t [s]	
0	3	3
1	14	7.5
5	55	12
10	120	42
20	565	277
25		847
30		1785
40		4785
50		9495

Table 2: HS and ZOHS validation using semi-discretization

Case	$f(t)$	Method	R	t	Approximation
Constant ω_{sv}	$a_{\mathrm{sv}}\sin(\omega_{\mathrm{sv}}t)$ and $a_{\mathrm{sv}}\,\mathrm{sgn}\big(\sin(\omega_{\mathrm{sv}}t)\big)$	SD	-	38 h	Reference
		ZOHS	10	2 min	Optimal
			5	55 s	Excellent
Constant PPTDR	$a_{\mathrm{sv}}\sin(PPTDR\,\omega_{\mathrm{T}}t)$	SD	-	112 min	Reference
		HS	50	160 min	Optimal
			40	80 min	Excellent
			10	42 s	Good

Table 3: Stiffness variation effect on milling stability

Case	$f(t)$	Method	Δa_{lim} [%]	Ω [rpm]
Constant ω_{sv}	$a_{\mathrm{sv}}\sin(\omega_{\mathrm{sv}}t)$	ZOHS	+110	2500
	$a_{\mathrm{sv}}\,\mathrm{sgn}\big(\sin(\omega_{\mathrm{sv}}t)\big)$		+170	2500
Constant PPTDR	$a_{\mathrm{sv}}\sin(PPTDR\,\omega_{\mathrm{T}}t)$	HS	+139	3500

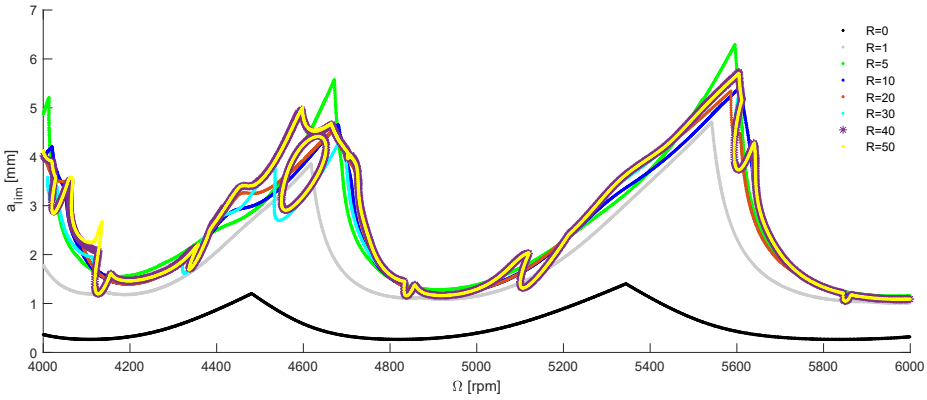

Fig. 7. Convergence analysis of HS with constant PPTDR stiffness variation (Eq. (24))

more harmonics considered, the more the computational time required as shown in Table 1. With $R = 1$ the absolute limit of stability is close to the real value but still far from the convergence. By increasing to $R = 5$ the lobes follow the final shape better, however the convergence is achieved between $R = 40$ and $R = 50$.

The solution is equivalent to that obtained using semi-discretization. Fig. 9 shows that the two stability lobes diagrams are in perfect agreement over the whole range of speeds. Considering a spindle speed range of between 4000 and 6000 rpm (Fig. 9) it is possible to see that HS is able to detect the instability island at about 4600 rpm. The computational time at convergence is close to that of semi-discretization evaluated with a discretization factor $k = 100$ (Table 2). However, good results were obtained considering 10 harmonics and the solution time is an order of magnitude faster than with semi-discretization.

In Fig. 10 and Table 3 the comparison between constant PPTDR stiffness variation and the equivalent LTI system is shown. The stability limit is more than doubled at low and medium spindle speeds. Therefore, an accurate design of asymmetric rotating parts leads to an increase of the productivity of the machine in the range of low and medium cutting speeds.

Overall, the efficiency of HS is almost equivalent to semi-discretization at convergence. However, in the frequency domain it is possible to neglect higher

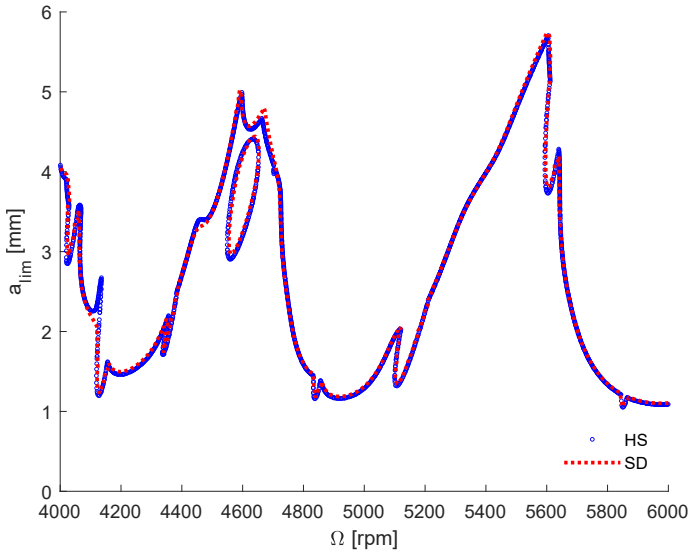

Fig. 8. Validation of HS: detection of island of instability

order harmonics, thereby abruptly reducing the computational time. With reference to the blue line in Fig. 7 computed with $R = 10$ harmonics, this shows a small loss of accuracy in the shape of the lobes and the identification of the island of instability is missing. Nevertheless, for practical applications it is a widely acceptable approximation. Under these conditions the solution took only 42 s to be evaluated compared to 112 min using semi-discretization. Consequently, HS can be a relevant tool for industrial applications and for conducting rapid analysis and optimization of LTP dynamics.

5. Conclusions

LTP system dynamics in milling applications are playing an important role in practical applications. The LTP dynamic can be due to the presence of asymmetric stiffness in rotating or stationary parts of the machine tool and workpiece. Moreover, the periodic modulation of the stiffness leads to the enhancement of the absolute stability limit at low and medium cutting speeds. This is a novel passive strategy to increase productivity in metal cutting, which is known as

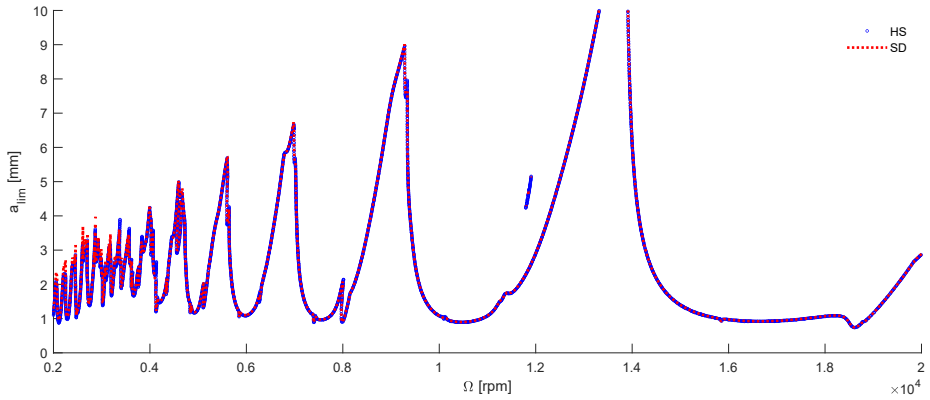

Fig. 9. Validation of HS with sinusoidal function and constant PPTDR stiffness variation over a wide spindle speed range

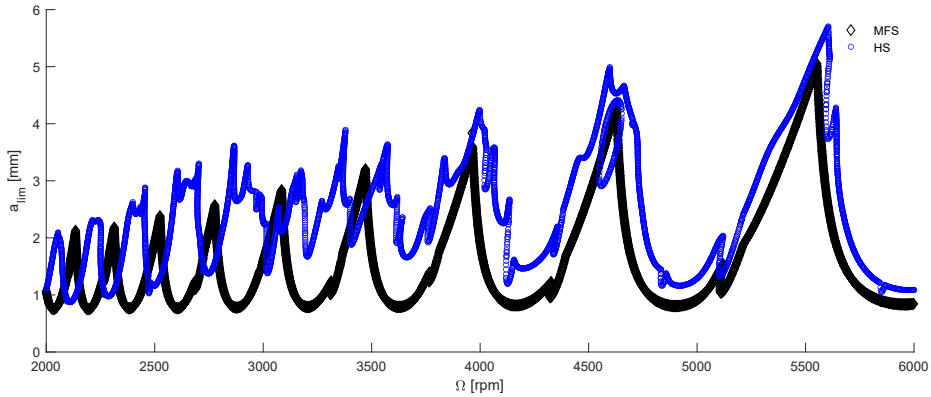

Fig. 10. Stability enhancement of constant PPTDR stiffness variation

stiffness variation and is gaining interest thanks to its potential. The traditional formulation of milling dynamics in the frequency domain can only deal with LTI systems, while time domain techniques are more general but time consuming and need a modal representation of the system. Thus, it is difficult to deal with in industries and they have found their application in research. In this paper the HS and the ZOHS are presented, which are two novel formulations in the frequency domain based on the LTP system theory. On one hand, HS is the most general solution which covers the contribution made by the LTP dynamics and the cutting process dynamics. Indeed, by managing the two matrices that make these contributions, it is possible to obtain the simplified ZOHS or the well known Multi Frequency Solution. The first considers the harmonics of the LTP dynamics and the constant contribution of the cutting dynamics, vice-versa the second considers the harmonics of the cutting dynamics and the LTI dynamics of the system. HS is able to give a precise prediction and is efficient in the presence of a small, integer and constant PPTDR. On the other hand, ZOHS considers only the average value of the cutting dynamics, giving rapid solutions in presence of a dynamic behaviour independent from the spindle rotation (i.e. constant frequency of stiffness variation). Stability lobes diagrams are given within 10 min on a commercial laptop, which is an order of magnitude faster than what it is possible to achieve using semi-discretization. HSs are based on the HTF, which can be experimentally identified and the results can be directly introduced in the algorithm. Moreover, the computational effort does not depend on the complexity of the dynamical system, which means that it is possible to deal efficiently with systems characterized by multiple critical modes. These characteristics fulfills the need of industrial applications and make the process of stiffness variation parameters optimization easier and faster.

6. Acknowledgments

This research was supported by Pama S.p.A. under an executive PhD program.

References

[1] T. Insperger, G. Stépán, Semi-discretization method for delayed systems, Int. J. Numer. Methods Eng. 55 (5) (2002) 503–518. doi:10.1002/nme.505.

[2] T. Insperger, G. Stépán, Updated semi-discretization method for periodic delay-differential equations with discrete delay, Int. J. Numer. Methods Eng. 61 (1) (2004) 117–141. doi:10.1002/nme.1061.

[3] Y. Ding, L. Zhu, X. Zhang, H. Ding, A full-discretization method for prediction of milling stability, Int. J. Mach. Tools Manuf. 50 (5) (2010) 502–509. doi:https://doi.org/10.1016/j.ijmachtools.2010.01.003.

[4] P. V. Bayly, J. E. Halley, B. P. Mann, M. A. Davies, Stability of interrupted cutting by temporal finite element analysis, J. Manuf. Sci. Eng. 125 (2) (2003) 220–225. doi:10.1115/1.1556860.

[5] G. Totis, P. Albertelli, M. Sortino, M. Monno, Efficient evaluation of process stability in milling with Spindle Speed Variation by using the Chebyshev Collocation Method, J. Sound Vib. 333 (3) (2014) 646–668. doi:10.1016/j.jsv.2013.09.043.

[6] Y. Altintaş, E. Budak, Analytical Prediction of Stability Lobes in Milling, CIRP Annals - Manuf. Technol. 44 (1) (1995) 357–362. doi:10.1016/S0007-8506(07)62342-7.

[7] S. D. Merdol, Y. Altintas, Multi Frequency Solution of Chatter Stability for Low Immersion Milling, J. Manuf. Sci. Eng. 126 (3) (2004) 459–466. doi:10.1115/1.1765139.

[8] D. Bachrathy, G. Stepan, Improved prediction of stability lobes with extended multi frequency solution, CIRP Annals 62 (1) (2013) 411–414. doi:10.1016/J.CIRP.2013.03.085.

[9] Y. Mohammadi, K. Ahmadi, Frequency domain analysis of regenerative chatter in machine tools with Linear Time Periodic dynamics, Mech. Syst. Signal Process. 120 (2019) 378–391. doi:10.1016/j.ymssp.2018.10.029.

[10] C.-J. Li, A. G. Ulsoy, W. J. Endres, The Effect of Flexible-Tool Rotation on Regenerative Instability in Machining, J. Manuf. Sci. Eng. 125 (1) (2003) 39–47. doi:10.1115/1.1536657.

[11] A. Comak, O. Ozsahin, Y. Altintas, Stability of Milling Operations With Asymmetric Cutter Dynamics in Rotating Coordinates, J. Manuf. Sci. Eng. 138 (8) (2016) 081004. doi:10.1115/1.4032585.

[12] M. Eynian, Y. Altintas, Analytical Chatter Stability of Milling With Rotating Cutter Dynamics at Process Damping Speeds, J. Manuf. Sci. Eng. 132 (2) (2010) 021012. doi:10.1115/1.4001251.

[13] D. J. Segalman, J. M. Redmond, Chatter suppression through variable impedance and smart fluids, in: Smart Structures and Materials 1996: Industrial and Commercial Applications of Smart Structures Technologies, 1996. doi:10.1117/12.239147.

[14] D. J. Segalman, E. A. Butcher, Suppression of regenerative chatter via impedance modulation, J. Vib. Control 6 (2) (2000) 243–256. doi:10.1177/107754630000600205.

[15] N. K. Garg, B. P. Mann, N. H. Kim, M. H. Kurdi, Stability of a Time-Delayed System With Parametric Excitation, J. Dyn. Syst. Meas. Control. 129 (2) (2007) 125–135. doi:10.1115/1.2432357.

[16] D. Mei, Z. Yao, T. Kong, Z. Chen, Parameter optimization of time-varying stiffness method for chatter suppression based on magnetorheological fluid-controlled boring bar, Int. J. of Advanced Manuf. Technol. 46 (2010) 1071–1083. doi:10.1007/s00170-009-2166-9.

[17] Z. Yao, D. Mei, Z. Chen, Chatter suppression by parametric excitation: Model and experiments, J. Sound Vib. 330 (13) (2011) 2995–3005. doi:10.1016/j.jsv.2011.01.031.

[18] Y. Liu, A. Fischer, P. Eberhard, B. Wu, A high-order full-discretization method using Hermite interpolation for periodic time-delayed differential equations, Acta Mech. Sin. 31 (3) (2015) 406–415. doi:10.1007/s10409-015-0397-6.

[19] Y. Sun, Z. Xiong, High-order full-discretization method using Lagrange interpolation for stability analysis of turning processes with stiffness variation, J. Sound Vib. 386 (2017) 50–64. doi:10.1016/j.jsv.2016.08.039.

[20] C. Wang, X. Zhang, Y. Liu, H. Cao, X. Chen, Stiffness variation method for milling chatter suppression via piezoelectric stack actuators, Int. J. Mach. Tools Manuf. 124 (2018) 53–66. doi:10.1016/j.ijmachtools.2017.10.002.

[21] C. Wang, X. Zhang, J. Liu, R. Yan, H. Cao, X. Chen, Multi harmonic and random stiffness excitation for milling chatter suppression, Mech. Syst. Signal Process. 120 (2019) 777–792. doi:10.1016/j.ymssp.2018.11.019.

[22] N. M. Wereley, Analysis and control of linear periodically time varying systems, Ph.D. thesis, Massachusetts Institute of Technology (1990).
URL https://dspace.mit.edu/handle/1721.1/13761

[23] S. Bittanti, P. Colaneri, Periodic systems: Filtering and control, in: Communications and Control Engineering, Springer, 2009.

[24] A. Siddiqi, Identification of the harmonic transfer functions of a helicopter rotor, Ph.D. thesis, Massachusetts Institute of Technology (2001).
URL https://dspace.mit.edu/handle/1721.1/8900

[25] M. S. Allen, M. W. Sracic, S. Chauhan, M. H. Hansen, Output-only modal analysis of linear time-periodic systems with application to wind turbine

simulation data, Mech. Syst. Signal Process. 25 (4) (2011) 1174–1191. doi:10.1016/j.ymssp.2010.12.018.

[26] D. Bachrathy, G. Stépán, Bisection method in higher dimensions and the efficiency number, Period. Polytech. Mech. Eng. 56 (2) (2012) 81–86. doi:10.3311/pp.me.2012-2.01.